◆ Human Brain Mapping 30:403–416 (2009) ◆

Small-World Properties of Nonlinear Brain Activity in Schizophrenia

Mikail Rubinov,[1,2]* Stuart A. Knock,[1] Cornelis J. Stam,[3] Sifis Micheloyannis,[4] Anthony W.F. Harris,[5,6] Leanne M. Williams,[5,6] and Michael Breakspear[1]

[1]*Black Dog Institute and School of Psychiatry, University of New South Wales, Sydney, Australia*
[2]*Schizophrenia Research Institute, Sydney, Australia*
[3]*VU University Medical Center, Amsterdam, The Netherlands*
[4]*Clinical Neurophysiology Research Laboratory, Medical Division, University of Crete, Iraklion, Crete, Greece*
[5]*Discipline of Psychological Medicine, Western Clinical School, University of Sydney, Australia*
[6]*Brain Dynamics Centre, Westmead Millennium Institute and Western Clinical School, University of Sydney, Westmead Hospital, Sydney, Australia*

Abstract: A disturbance in the interactions between distributed cortical regions may underlie the cognitive and perceptual dysfunction associated with schizophrenia. In this article, nonlinear measures of cortical interactions and graph-theoretical metrics of network topography are combined to investigate this schizophrenia "disconnection hypothesis." This is achieved by analyzing the spatiotemporal structure of resting state scalp EEG data previously acquired from 40 young subjects with a recent first episode of schizophrenia and 40 healthy matched controls. In each subject, a method of mapping the topography of nonlinear interactions between cortical regions was applied to a widely distributed array of these data. The resulting nonlinear correlation matrices were converted to weighted graphs. The path length (a measure of large-scale network integration), clustering coefficient (a measure of "cliquishness"), and hub structure of these graphs were used as metrics of the underlying brain network activity. The graphs of both groups exhibited high levels of local clustering combined with comparatively short path lengths—features consistent with a "small-world" topology—as well as the presence of strong, central hubs. The graphs in the schizophrenia group displayed lower clustering and shorter path lengths in comparison to the healthy group. Whilst still "small-world," these effects are consistent with a subtle randomization in the underlying network architecture—likely associated with a greater number of links connecting disparate clusters. This randomization may underlie the cognitive disturbances characteristic of schizophrenia. *Hum Brain Mapp 30:403–416, 2009.* © 2007 Wiley-Liss, Inc.

Key words: schizophrenia; connectivity; EEG; nonlinear dynamics; graph theory; small-world network

Contract grant sponsor: SRI summer student scholarship; Contract grant sponsor: Brain NRG; Contract grant number: JSM22002082; Contract grant sponsor: ARC; Contract grant numbers: DP0667065, TS0669860.

*Correspondence to: Mikail Rubinov, School of Psychiatry, University of New South Wales, Black Dog Institute, Hospital Road, Randwick, New South Wales, 2031, Australia.
E-mail: m.rubinov@student.unsw.edu.au

Received for publication 14 August 2007; Accepted 11 October 2007
DOI: 10.1002/hbm.20517
Published online 10 December 2007 in Wiley InterScience (www.interscience.wiley.com).

INTRODUCTION

Dynamic interactions between distributed cortical regions may integrate the disparate aspects of a cognitive process into a perceptual whole [Roskies, 1999]. A disruption of such interactions may therefore underlie the cognitive [Andreasen, 1999; Friston and Frith, 1995; Lee et al., 2003; Peled, 1999] and behavioral [Williams et al., 1999] disturbances of schizophrenia. This "disconnection hypothesis" resonates with Bleuler's [1911/1950] observation that schizophrenia interrupts "the associative threads which

guide our thinking." Disconnectivity has been implicated in cortico-limbic [Das et al., in press], cortico-thalamic [Tononi and Edelman, 2000], and cortico-thalamic-cerebellar [Andreasen et al., 1996] circuits, and their structural underpinnings [Bullmore et al., 1997; Woodruff et al., 1997]. The term disconnectivity has hence been used to infer disturbances in both spatial and temporal cortical coordination. Whereas spatial disjunctions may underlie the emergence of incongruent associations (such as "inappropriate affect"), disturbances in temporal coordination may lead to the disruptions in the stream of thoughts (such as "derailment"). Hence, the symptoms of schizophrenia may not simply reflect a disconnection of concurrent cortical processes but also a disturbance in the temporal transition between sequential processes, namely "cognitive dysmetria" [Andreasen et al., 1999]. Here we investigate the disconnection hypothesis through nonlinear and graph-theoretical analysis of resting state EEG acquired during a first episode of schizophrenia. We employ a measure which is sensitive to both the spatial and temporal aspects of cortical interdependence, in order to be optimally sensitive to the cognitive disturbances of schizophrenia.

Our connectivity analysis is based upon the estimation of "nonlinear interdependence" between pairs of electrodes taken from a scalp-wide array. This measure assesses the degree to which the current state of one dynamical system predicts the future activity of another [Schiff et al., 1996; Terry and Breakspear, 2003]. Past EEG studies of schizophrenia have usually employed linear measures [Haig et al., 2000; Spencer et al., 2003; Symond et al., 2005]. Nonlinear processes are strongly present during seizures [Arnhold et al., 1999; Breakspear et al., 2006; Perez-Velazquez and Khosravani, 2004], occur intermittently in healthy resting state EEG [Breakspear and Terry, 2002a; Stam et al., 1999] and may underlie motor coordination [Jirsa et al., 1998; Meyer-Lindenberg et al., 2002]. Nonlinear variation in symptom expression has been observed in schizophrenia [Tschacher et al., 1997] and bipolar disorder [Gottschalk et al., 1995]. Furthermore, nonlinear interactions encompass interdependences between activity at different timescales [Breakspear, 2004; Friston, 2001; Rabinovich et al., 2006; Schanze and Eckhorn, 1997]. These considerations motivate the use of nonlinear methods to investigate the schizophrenia disconnection hypothesis [Breakspear, 2006].

We previously employed these nonlinear techniques across a restricted array of scalp electrodes to study cortical interactions in schizophrenia in a resting state condition [Breakspear et al., 2003]. Surprisingly, there was no significant between-group difference in the occurrence of nonlinear interdependence between any pair of recordings. However, we did observe a strong between-group difference in the relative timing of nonlinear interdependence. Specifically, in schizophrenia, we observed an increase in the concurrent expression of interdependences. That is, there was a bias towards clusters of cooccurring nonlinear interdependence in schizophrenia, and away from isolated pair-wise occurrences. This bias became further pronounced hierarchically, up to the scale of the whole electrode array.

What is the nature of the underlying network structure of nonlinear interdependence in schizophrenia? This question requires additional techniques suited to the analysis of complex network structure. In the present study we reanalyze the above data set of resting state EEG by employing the methods of graph theory (and after expanding our array to cover the entire available array of scalp electrodes). A graph, composed of nodes and edges, represents a network (Fig. 1A,C). Graph-theoretical metrics such as clustering coefficient, characteristic path length and centrality (Fig. 1B) allow one to quantify both local and global attributes of network topology. The clustering coefficient characterizes the presence of highly interconnected groups of nodes ("cliques"). Path length measures the average shortest distance between any two nodes. Centrality (or "betweenness") detects "hubs"—central nodes which participate in a large proportion of shortest paths. These measures are ideal for understanding complex networks such as the brain [Bassett and Bullmore, 2006; Sporns and Zwi, 2004].

It has been proposed that the brain's overall network structure optimizes the interplay between the segregation and integration of functionally specialized areas [Tononi et al., 1994]. This interplay is well conceptualized by the highly clustered, yet globally interconnected "small-world" networks [Watts and Strogatz, 1998]. Such networks have been described in cortical anatomy [He et al., 2007; Sporns and Zwi, 2004; Stephan et al., 2000] and in EEG and MEG studies, where a disturbed small-world pattern has been reported in patients with brain tumors [Bartolomei et al., 2006], Alzheimer's disease [Stam et al., 2007] and epilepsy [Ponten et al., 2007], as reviewed in Bassett and Bullmore [2006] and Stam and Reijneveld [2007]. Therefore, assuming an optimal small-world-like topology in health, brain network analysis may advance the schizophrenia disconnection hypothesis through a quantitative characterization of disconnections as well an assessment of their impact on global topographic properties of the cortical system. In keeping with this, Micheloyannis et al. [2006] recently reported a reduction in the small-world properties of cortical networks in schizophrenia during the performance of a two-back working memory task. In the present study we address resting state networks, whose importance to cognitive networks is a subject of increasing interest [e.g. Greicius et al., 2003], hence complementing the findings from this active (memory) task.

MATERIALS AND METHODS

The subjects and preliminary data analysis have been previously described [Breakspear et al., 2003] but are provided here for completeness. Subject recruitment and data acquisition was conducted at the Brain Dynamics Centre, Westmead Hospital as part of the Western Sydney First Episode Psychosis Project [Harris et al., 2005].

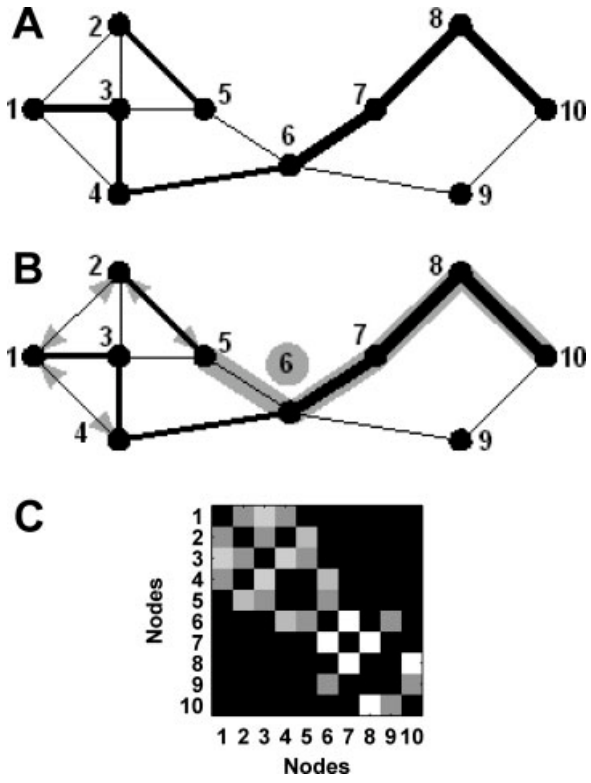

Figure 1.

(**A**) A graph is a basic representation of a network: as a minimum it comprises a collection of nodes (numbered), connected to each other by edges (lines). In weighted graphs, each edge is assigned a value reflecting the strength of the connection (line widths). (**B**) An illustration of network metrics used in this article. The shortest path between Nodes 5 and 10 is shaded (note that stronger weights correspond to shorter path lengths). Node 6 (circled) is a "hub"—a central node that is traversed by ~50% of shortest paths in the network. The binary clustering coefficient for Node 3 equates to the number of edges connecting neighbors of 3, as a proportion of the total possible number of such edges. There are three present "neighbor–neighbor" edges (arrowheads) out of a possible six—yielding a binary clustering coefficient of 0.5. A calculation of weighted clustering coefficient will, in addition, incorporate weights of edges that connect Node 3 to its neighbors (for example: given that edges 3↔1 and 3↔4 have greater weights than 3↔2 and 3↔5, this will mean that the presence of edge 1↔4 will increase the weighted clustering coefficient to a greater extent than the presence of edge 2↔5). (**C**) A weights matrix representation of the graph in 1A. Squares represent connections between nodes (edges); brightness of squares corresponds to edge weights.

Subjects and Clinical Assessment

Clinical subjects were 40 young individuals (26 male, 14 female) aged between 14 and 26 years (mean = 19.6; SD = 3.2) who had presented for the first time to health services with psychotic symptoms that warranted a diagnosis of either schizophrenia or schizophreniform disorder. Following a semi-structured interview with the SCID, diagnosis was made according to DSM-IV [American Psychiatric Association, 1994] by means of a consensus conference (of at least three qualified psychiatrists) that drew upon a clinical interview and family, case manager and case note information. Subjects were clinically assessed usually on the day of their EEG recording (and never more than three days before) by trained psychiatrists (interrater reliability >0.80) according to the positive and negative syndrome scale (PANSS) [Kay et al., 1986]. This was a relatively young and acutely ill clinical group (Table I). Inclusion criteria were psychotic symptoms as defined by a rating of four or more on items relating to psychosis on the PANSS. The majority of subjects were receiving atypical antipsychotic medications (mean = 250 chlorpromazine equivalents; SD = 202). Four participants were on no medication. The 40 healthy control subjects, recruited from similar demographic regions, were matched for sex and age (to within 24 months: mean = 19.7; SD = 3.9). The exclusion criterion for controls was a history of psychiatric illness (themselves or first-degree relative). Exclusion criteria for all subjects were a history of neurological disease, head injury, developmental delay, left handedness, and substance dependence. All subjects gave voluntary and informed consent according to national health and medical research council guidelines. The study had local institutional ethics approval.

Acquisition of EEG

EEG data were acquired whilst subjects were instructed to rest with eyes open and look at a stationary dot on a monitor. An electrode cap was used to acquire data from the international 10–20 system of scalp sites and linked earlobes served as the reference. Skin resistance at each site was <5 kΩ. EEG data were collected for 130 s at a rate of 250 Hz through a SynAmps^{TM} amplifier and filtered with a 50 Hz low-pass third order Butterworth filter. Artifacts caused by eye movement were corrected offline according to the method of Gratton et al. [1983]. To avoid confounding of interelectrode coherence by the effects of a common reference electrode, close bielectrode derivations were used [Nunez et al., 1997]. Seven bipolar deriva-

TABLE I. Average PANSS for the 40 clinical subjects

P1	P2	P3	P4	P5	P6	P7
3.05	2.32	2.57	2.33	1.93	2.83	2
N1	N2	N3	N4	N5	N6	N7
2.88	2.9	2.38	2.73	3.85	2.68	2.13

P1, delusions; P2, conceptual disorganization; P3, hallucinatory behavior; P4, excitement; P5, grandiosity; P6, suspiciousness; P7, hostility; N1, blunted affect; N2, emotional withdrawal; N3, poor rapport; N4, passive/apathetic; N5, diminished abstract thinking; N6, loss of spontaneity; N7, stereotypical thinking.

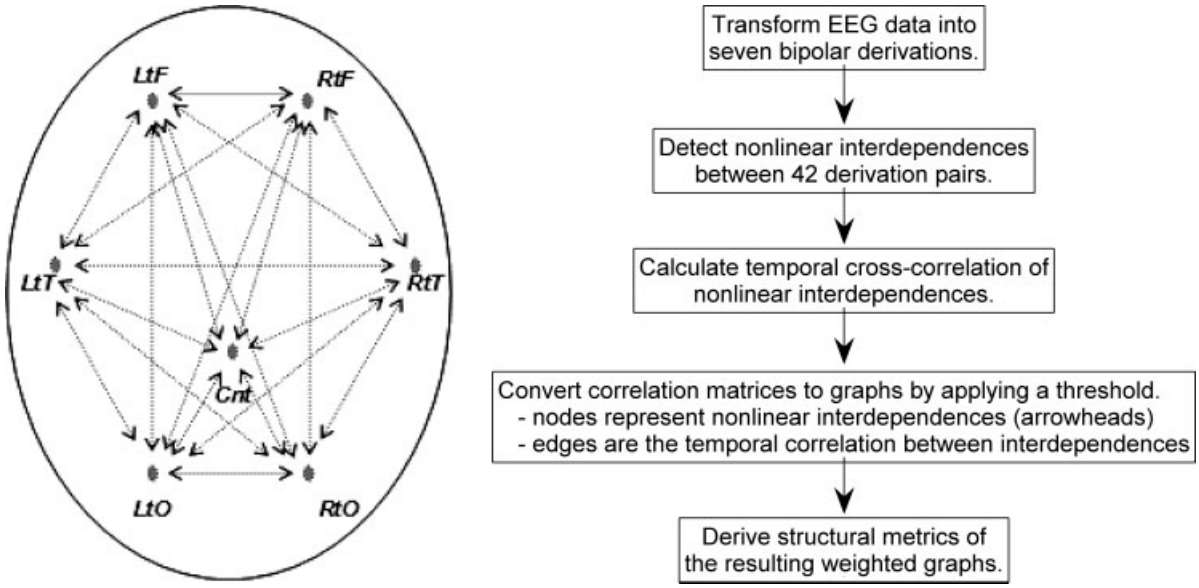

Figure 2.

A summary of the data analysis methodology and a schematic representation of bipolar electrode derivation positions and their pair-wise interactions. Key: left frontal (LtF) = F3C3 derivation, right frontal (RtF) = F4C4, left temporal (LtT) = T3T5, right temporal (RtT) = T4T6, left occipital (LtO) = O1P3, right occipital (RtO) = O2P4, Central (Cnt) = CzPz.

tions—representing left and right (frontal, temporal and posterior) and central cortical regions—were included in the analysis. All possible pair-wise interactions between these were calculated. A schema of the location of these bipolar derivations is presented in Figure 2.

Data Analysis

There are three steps to the analysis. In the first step, the presence of transient nonlinear interdependence between each pair of bipolar derivations was assessed over short (2.048 s) windows of data. In the second step, the spatio-temporal properties of these nonlinear interdependences were represented as graphs. In the third step, structural properties of such graphs—for each subject—were derived and between-group comparisons of these graph properties were then performed. Figure 2 presents a summary of the data analysis methodology.

Step 1: Detection of dynamical interdependence between electrode pairs

All pair-wise combinations of electrodes were examined for evidence of nonlinear interdependence according to the procedure modified from the algorithm of Schiff et al. [1996]. The algorithm takes a geometric approach to time series analysis, optimizing standard nonlinear forecasting algorithms. Its validation, together with the rationale for the choice of the analysis parameters, are described elsewhere [Breakspear and Terry, 2002a,2002b; Terry and Breakspear, 2003]. A brief description follows.

Each electrode pair yields two time series of 130 s duration for each subject. These time series were analyzed in sequential windows of 2.048 s duration. This window length enables a robust detection of nonlinearity, whilst also being sufficiently short to capture their transient temporal character [Terry and Breakspear, 2003]. The power of two sample length optimizes the computational speed. In each window, two "nonlinear crossprediction errors" were calculated. Each error reflects the ability of a nonlinear model constructed from one time series to predict the amount of uncertainty in the other time series. Low errors indicate a good crossprediction and hence nonlinear structure in the relationship between the two time series. Using a nonparametric bootstrap scheme (applied to the original data), an ensemble of prediction errors is then calculated. These represent the null hypothesis that the values of the errors are due to purely linear correlations between the two time series [Prichard and Theiler, 1994; Rombouts et al., 1995]. The data is said to contain nonlinear interdependence if the observed (experimentally derived) prediction error lies outside of the distribution of these "surrogate" errors. Nineteen surrogates were constructed to allow for nonparametric statistical inference at 95% confidence within each window.

Step 2: The topography of nonlinear interdependence across multiple sites

For each electrode pair and in each direction, this procedure generated a second-level time series indicating the presence or absence of nonlinear interdependence in each

successive epoch. For each subject there are 58 epochs and 21 sets of pairs, with two directions between each pair, hence yielding 42-time series of length 58-time points (corresponding to 58 windows). These time series represent the fluctuating nature of spatial interactions—as captured through nonlinear techniques. The temporal character of these interactions was captured by calculating the temporal cross-correlation functions between these time series [Breakspear and Terry, 2002b]. This contrasts with the alternative approach of calculating the average spatial interdependence across all available time windows, thus approximating the "expected" interdependence whilst filtering out their specific temporal character.

For each subject this approach yields 861 unique correlation coefficients (from the 42 × 42 correlation matrix). Graph analytic techniques are applied to these 42 × 42 matrices. Each graph contains information about both the spatial and temporal expression of nonlinear interdependence between cortical regions. There are 40 of these graphs in both the control and clinical data sets.

Step 3: Graph-theoretical analysis of the correlation matrices

Graph analysis was performed in Matlab (The MathWorks, Inc.) with software written by one of the authors (MR). Correlation matrices were converted to graphs by applying a range of thresholds—from 10 to 30% of the strongest edges preserved. This enabled comparison of the structural pattern of graphs irrespective of the overall between-group difference in the weights and across a range of graph-connectedness (as there is no natural threshold to use).

The weighted clustering coefficient [Barrat et al., 2004] was calculated individually for each node and subsequently averaged over the graph. It is a modified binary clustering coefficient [Watts and Strogatz, 1998]. For any Node A, we consider all neighbors of A (nodes directly connected to A) and all neighbor–neighbor edges (connections between pairs of neighbors). The binary clustering coefficient is the ratio of all present neighbor–neighbor edges to the maximum possible number of such edges. The weighted clustering coefficient, in addition, incorporates the weights of node–neighbor edges into the calculations (Fig. 1B). Both coefficients range from 0 to 1. Characteristic path length was calculated by averaging the shortest path lengths between all pairs of nodes, with the weights of edges taken to be inversely proportional to the path length. Centrality [Freeman, 1977] was calculated individually for each node. For any Node A, we first obtain the proportion of all B→C shortest paths that traverse A. Subsequently we sum these proportions over all B/C pairs and normalize by the number of these pairs (hence centrality ranges from 0 to 1). Formal definitions of the clustering coefficient, characteristic path length and centrality are provided in the appendix.

We previously found that weak correlations of nonlinear interdependence were not statistically significant [Breakspear and Terry, 2002a]. Therefore by removing these weak edges through thresholding we are better able to elicit any underlying nonrandom structure. However, removing too many edges will disconnect the graphs, thus imposing limitations on the calculation of path length and centrality. We overcame this problem for path lengths by calculating the harmonic, rather than the arithmetic mean [Marchiori and Latora, 2000; Newman, 2003]—this effectively negates the effects of any disconnected node pairs. However for calculations of centrality it is the number of paths, rather than the path length, that is important. As a graph disconnects into multiple components, the number of paths sharply drops, thus obscuring individual node centralities. To enable a more accurate estimation of centrality we constructed sparse and connected graphs through retaining all "bridges"—edges, which if removed, would split the graph into more than one component—irrespective of the weight of the bridge. This approach recognizes that the underlying spatiotemporal brain networks are likely to contain paths between all regions, and that their apparent disconnections are an artifact of our sparse spatial data sampling. The number of extra preserved bridges was not statistically different between the two groups at any of the examined thresholds, hence being an unlikely source of bias for the estimation of node centrality.

To account for differences in weight and degree distributions between subjects—which may have a confounding effect on graph metrics—all measures were compared to those derived from corresponding "surrogate" random graphs with equivalent weight and degree distributions [Sporns and Zwi, 2004]. Surrogate random graphs were created on a subject-wise basis as follows [Maslov and Sneppen, 2002]: pairs of edges (↔) were randomly selected, such that $node_A \leftrightarrow node_B$ and $node_C \leftrightarrow node_D$. The pairs were then rewired, such that $node_A \leftrightarrow node_D$ and $node_C \leftrightarrow node_B$ (rewiring did not proceed if either of the putative new edges already existed). This approach, in addition to preserving the exact binary degree, closely approximated the weighted degree of the original networks.

The comparison between observed and random graph measures was achieved—within each subject—by calculating a normalized graph statistic m_{nml} according to the formula: $m_{nml} = m_{obs}/m_{rand}$; where m is any of the metrics considered, m_{obs} is the observed value and m_{rand} is the average from 20 surrogate graphs [Milo et al., 2002]. Small-world networks typically have $C_{nml} \gg 1$, and $L_{nml} \approx 1$ where C is clustering and L path length. Therefore we used the index C_{nml}/L_{nml} to evaluate the small-world-ness of a network [Humphries et al., 2006]; for small-worlds we expect $C_{nml}/L_{nml} \gg 1$.

RESULTS

Average Correlation Coefficients and Average Thresholded Correlation Matrices

Figure 3A shows the rank-ordered average correlation coefficients for unthresholded correlation matrices of both

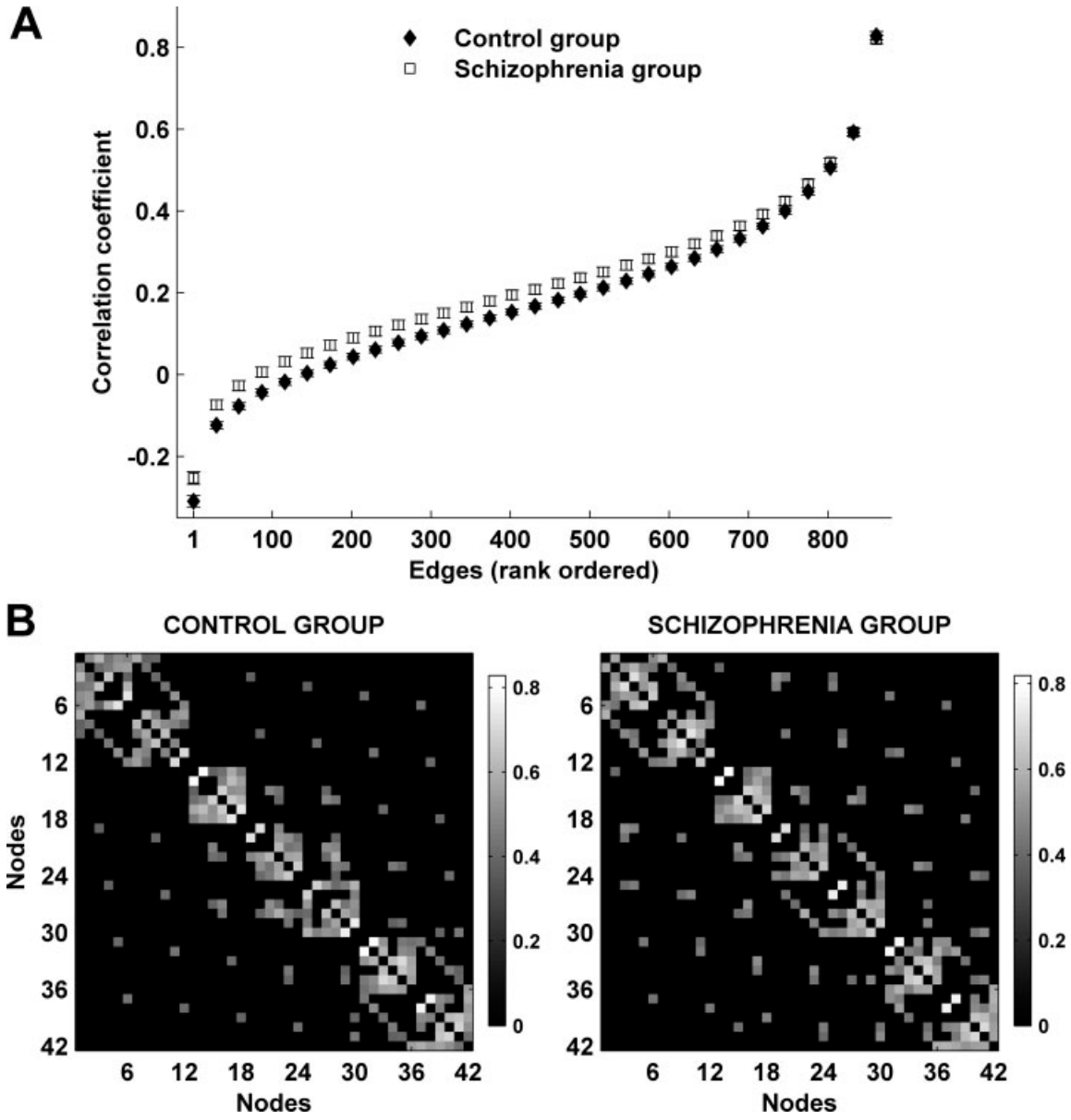

Figure 3.

(**A**) Edges from mean unthresholded correlation matrices of both subject groups rank-ordered by values of correlation coefficients. There are a total of 861 unique correlations in each unthresholded correlation matrix. The strongest 10–30% of these coefficients are considered for subsequent graph analysis. Correlation coefficients in schizophrenia are on average greater than in the control group for a range of rank-ordered means. (**B**) The average correlation matrices of both subject groups thresholded such that only 15% of the strongest weights are preserved. Both graphs are characterized by the presence of clusters and intercluster edges; the number of intercluster edges is greater in schizophrenia.

groups. Two findings are of note. First, most correlation coefficients range between −0.2 and 0.2: based on previous analysis, these are likely to contain a high proportion of chance values [Breakspear and Terry, 2002a]. Moreover, they capture only a small amount of the common variance (the square of the correlation coefficient <4%) in the underlying dynamics. For the subsequent analysis we consider the 10–30% of the strongest correlations which are hence more likely to reflect the underlying network architecture. Second, there is a prominent increase in the correlation coefficients in the schizophrenia group—this finding is consistent with the results of Breakspear et al. [2003] although expanded to a much larger data set studied here. For the ensuing analysis, this between-group difference is

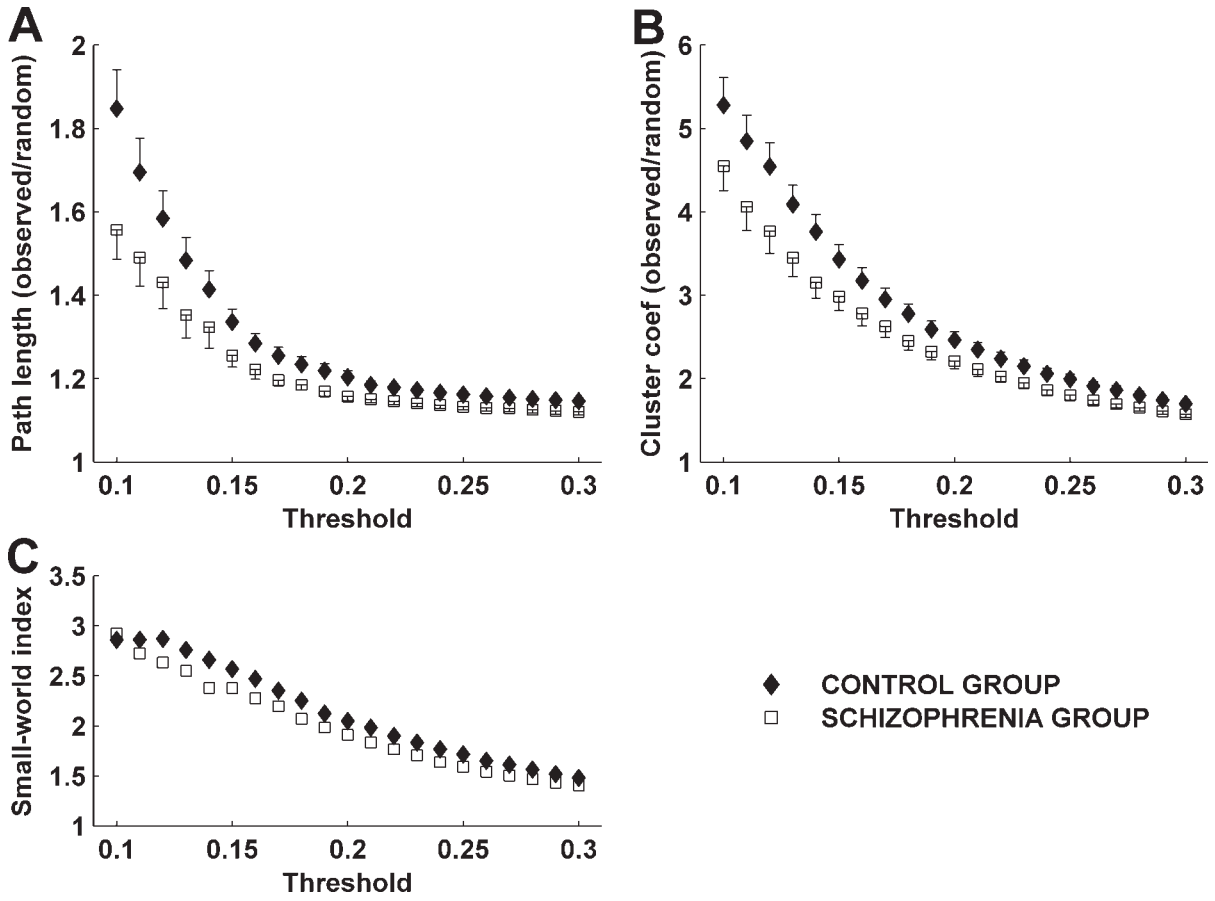

Figure 4.

Mean normalized path length (**A**) and clustering coefficients (**B**) at thresholds 10–30%. (**C**) The small-world index derived as C_{nml}/L_{nml} where C_{nml} is normalized clustering and L_{nml} is normalized path length. Small-world networks typically have $C_{nml}/L_{nml} \gg 1$.

controlled for by thresholding the graphs to have the same number of edges and then normalizing each subject's graph against surrogate graphs with equivalent weight distributions (i.e. constructed on a subject-wise basis).

Figure 3B shows the average correlation matrices for the two groups, thresholded such that 15% of the strongest edges are present. Our results were derived from graphs of individual subjects; however the average matrices roughly reproduce our findings and are illustrative of the typical network structure in both groups. A feature of both matrices is the presence of seven reasonably distinct clusters along the diagonal, each consisting of six adjacent nodes. Each cluster represents a group of interdependences originating from one bi-electrode derivation site. Therefore, interdependences originating from the same site are well correlated with each other. The location of off-diagonal edges near these clusters indicates that the first two clusters (from the left upper corner), the next three clusters, and the last two clusters are more interconnected between each other, thus forming three bigger, but "looser," clusters. These three clusters correspond to frontal, centro-temporal and posterior interdependences respectively. In addition both matrices feature fairly uniformly distributed peripheral edges (single edges well away from the diagonal) which serve the role of intercluster "shortcuts." These features were present to a varying extent in all subjects of both groups and are characteristic of a small-world network structure. A crucial between-group difference is the greater occurrence of peripheral edges, and consequently a reduced amount of edges within clusters, in the schizophrenia average graph. This is suggestive of a network structure with lower clustering and a shorter path length—a finding replicated by the consequent quantitative analysis.

Clustering Coefficient, Characteristic Path Length, and Centrality

Figure 4A,B show the average normalized clustering coefficients and characteristic path lengths in both groups

TABLE II. Clustering coefficient and path length

Threshold	Clustering coefficient	Path length
0.10	0.081	**0.007**
0.11	**0.044**	**0.016**
0.12	**0.031**	**0.014**
0.13	**0.037**	**0.007**
0.14	**0.027**	**0.021**
0.15	0.081	**0.015**
0.16	0.060	**0.010**
0.17	0.071	**0.011**
0.18	**0.037**	**0.012**
0.19	**0.041**	**0.006**
0.20	**0.036**	**0.005**
0.21	**0.041**	**0.006**
0.22	0.057	**0.008**
0.23	**0.046**	**0.005**
0.24	**0.019**	**0.005**
0.25	**0.029**	**0.004**
0.26	**0.025**	**0.005**
0.27	**0.017**	**0.006**
0.28	**0.029**	**0.004**
0.29	**0.022**	**0.004**
0.30	**0.032**	**0.005**
AUC	**0.025**	**0.0092**

Between-group *P*-values as a function of the fraction if edges preserved (Wilcoxon rank-sum test). AUC, area under curve analysis. Significant results are in bold.

plotted against thresholds of 10–30% of strongest edges. The between-subject (within group) variance is used to estimate the standard error of the mean. We note that greater between-group separation occurs as more edges were removed. However, this is also accompanied by some increase in the standard error. The rapid increase of the characteristic path length for the sparser graphs corresponds to the onset of graph disconnection.

The schizophrenia group demonstrates shorter path lengths and lower clustering coefficients across all thresholds. Table II shows the statistical significance of these between-group differences, assessed at each threshold by means of a Wilcoxon rank sum test (as the distributions were not Gaussian). The difference in path length is significant at $P < 0.05$ at all 21 thresholds. The difference in clustering is significant at 16 of the 21 thresholds. It is important to note that the graph measures derived from graphs with different thresholds are far from independent measures. Hence we provide the uncorrected *P*-values at each threshold. However, by calculating the area under the curve for each measure—a nonparametric means of assessing effects which vary across a range of dependent measures—we find robust between group differences. For the clustering coefficient the mean (±SEM) for the control group was 56.2 (±2.5), and for the schizophrenia group 49.3 (±2.3), corresponding to a significant between group effect ($P = 0.025$). The corresponding values for the path length were 25.7 (±0.45) and 24.3 (±0.41), a strong between group difference ($P = 0.0092$). This reduction in both path length and clustering coefficient is consistent with a randomization of the small-world network structure in schizophrenia [Watts and Strogatz, 1998], a point which we discuss in more detail below.

Another notable finding is that networks in both groups manifest small-world properties. At all thresholds the clustering coefficient is considerably larger than in the corresponding random graphs, whereas the path length stays reasonably close to the random graph path length. This is formally illustrated by the small-world index (Fig. 4C). We observe that the small-world effect is more prominent in the sparser graphs. Conversely, as more edges are retained, the small-world indices from both groups converge towards the null value of 1 (i.e. equivalent to a random network). This is consistent with our prior argument that weaker edges are more likely to contain chance (random) effects. The between group difference in this index is relatively weak (in comparison to the individual graph metrics) because the reduction in clustering coefficient in the schizophrenia group is largely offset by the corresponding reduction in path length.

The finding of a randomized network structure in the schizophrenia group is further supported by a between-group comparison of centrality (obtained from connected graphs, as discussed in the Methods). To ensure the analysis is sensitive to the presence of hubs, even if the hub location varies between subjects, centrality indices were rank-ordered within each subject. Figure 5A shows rank-ordered node centralities at threshold 12%, with comparative centralities of surrogate random networks. First, note that in distinction to the surrogate graphs, both the healthy and clinical data feature a considerably more heterogeneous centrality distribution, with the presence of a few prominent central hubs in each subject. This distribution roughly follows a power-law, which is consistent with previous analyses of the centrality [Newman, 2003], but has not been previously reported in schizophrenia. Repeating our analysis without the rank-ordering step annuls this property (Fig. 5B), arguing that there was no consistent topographical hub distribution across different subjects. Secondly, hub centrality in schizophrenia is significantly lower in comparison to the control group. Lower centrality of hubs corresponds to a greater diversity of shortest paths in the networks, which may occur as a result of a greater number of intercluster shortcuts. This is further supported by the observation that centrality of hubs—and the corresponding between-group difference—decreases as graphs become less sparse (the difference becomes nonsignificant at the 16% threshold).

Correlation of Schizophrenia Network Structure With Medication Dose and Symptom Ratings

Table III shows the values of Pearson's correlation coefficient for an exploratory analysis of the relationship between the clinical subjects' antipsychotic dose (in chlorpromazine equivalents) and symptom ratings (PANSS) against path lengths and clustering coefficients—at threshold 20%. Path lengths were not significantly correlated

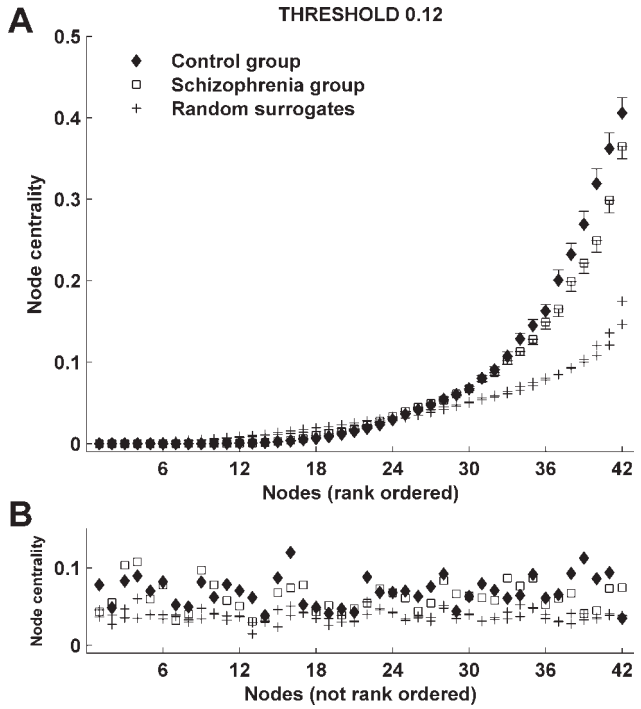

Figure 5.

(**A**) Mean rank-ordered centrality indices of individual nodes in both groups at threshold 12%. Centrality was obtained from connected sparse graphs using a bridge-preservation thresholding algorithm, as described in the Methods. Simple thresholding leads to disconnected graphs, significantly reducing the number of paths, thus obscuring individual node centralities (not shown). (**B**) Mean centrality indices in 5A, plotted without rank-ordering by node.

with medication dose at this threshold. Clustering coefficients, however, showed a significant positive correlation ($P = 0.009$): that is, medication dose was correlated against the between-group effect on this graph metric. Given that medication dose is related to disease expression, these correlations were recalculated using the partial correlation coefficient, with separate partialling out of the aggregate positive and negative symptom ratings. The significance of correlations remained unchanged (Table IV), suggesting that disease severity was not a confounder. There were few significant correlations between PANSS and graph indices. These included positive correlations between path length and N6 ($P = 0.031$) and N7 ($P = 0.016$), as well as a positive correlation between clustering and P1 ($P = 0.022$).

Comparison of Weighted and Unweighted Network Structure

To determine whether the distribution of the weights in our graphs provides information additional to the network topology, we recalculated the graph metrics after converting the matrices into binary graphs, achieved by setting supra-threshold edges to one. Figure 6A shows the normalized path length of binary graphs. A notable difference, when compared with weighted networks (Fig. 4A), is the overall reduction in path length in both groups, and a less prominent between-group difference—especially as the graphs become more densely connected. This is clearly illustrated at thresholds 20–30% (Fig. 6B)—the between-group effect remains robust in the weighted graphs, but is not present in the binary networks. Path length differences in binary graphs were only statistically significant at four out of 21 thresholds (10–13%).

Figure 6C,D show the clustering coefficient and centrality indices recalculated for binary graphs. Clustering in both groups, and the between-group clustering difference was similarly reduced in unweighted networks, but to a lesser extent. The difference in clustering coefficient was statistically significant at 12 out of 21 thresholds (11–14%, 19%, 21%, 24–29%). These additional analyses show that the weighted graph metrics behave in a qualitatively similar manner to the more-often used binary graphs but have

TABLE III. Correlation of network structure with medication dose (Med) and PANSS at threshold 0.20

Clustering coefficient	Correlation coefficient	*P* value	Path length	Correlation coefficient	*P* value
Med	**0.406**	**0.009**	Med	0.259	0.107
P1	**0.361**	**0.022**	P1	0.084	0.607
P2	0.031	0.851	P2	0.154	0.342
P3	0.028	0.866	P3	−0.012	0.939
P4	−0.010	0.951	P4	−0.060	0.324
P5	−0.033	0.840	P5	−0.067	0.682
P6	0.119	0.466	P6	0.024	0.882
P7	0.117	0.474	P7	0.133	0.412
N1	0.166	0.305	N1	0.282	0.078
N2	−0.028	0.863	N2	0.112	0.492
N3	0.137	0.400	N3	0.270	0.092
N4	0.022	0.891	N4	0.241	0.134
N5	0.184	0.256	N5	0.285	0.075
N6	0.109	0.505	N6	**0.342**	**0.031**
N7	−0.015	0.927	N7	**0.380**	**0.016**

Significant correlations are in bold.

TABLE IV. Partial correlation coefficients between network metrics and medication dose (Med) at threshold 0.20, with partialling out of aggregate positive (PSS) or aggregate negative (NSS) symptom ratings

	Clustering coefficient vs. Med		Path length vs. Med	
	Controlled for PSS	Controlled for NSS	Controlled for PSS	Controlled for NSS
Correlation coefficient	**0.409**	**0.413**	0.259	0.293
P value	**0.010**	**0.009**	0.112	0.070

Significant correlations are in bold.

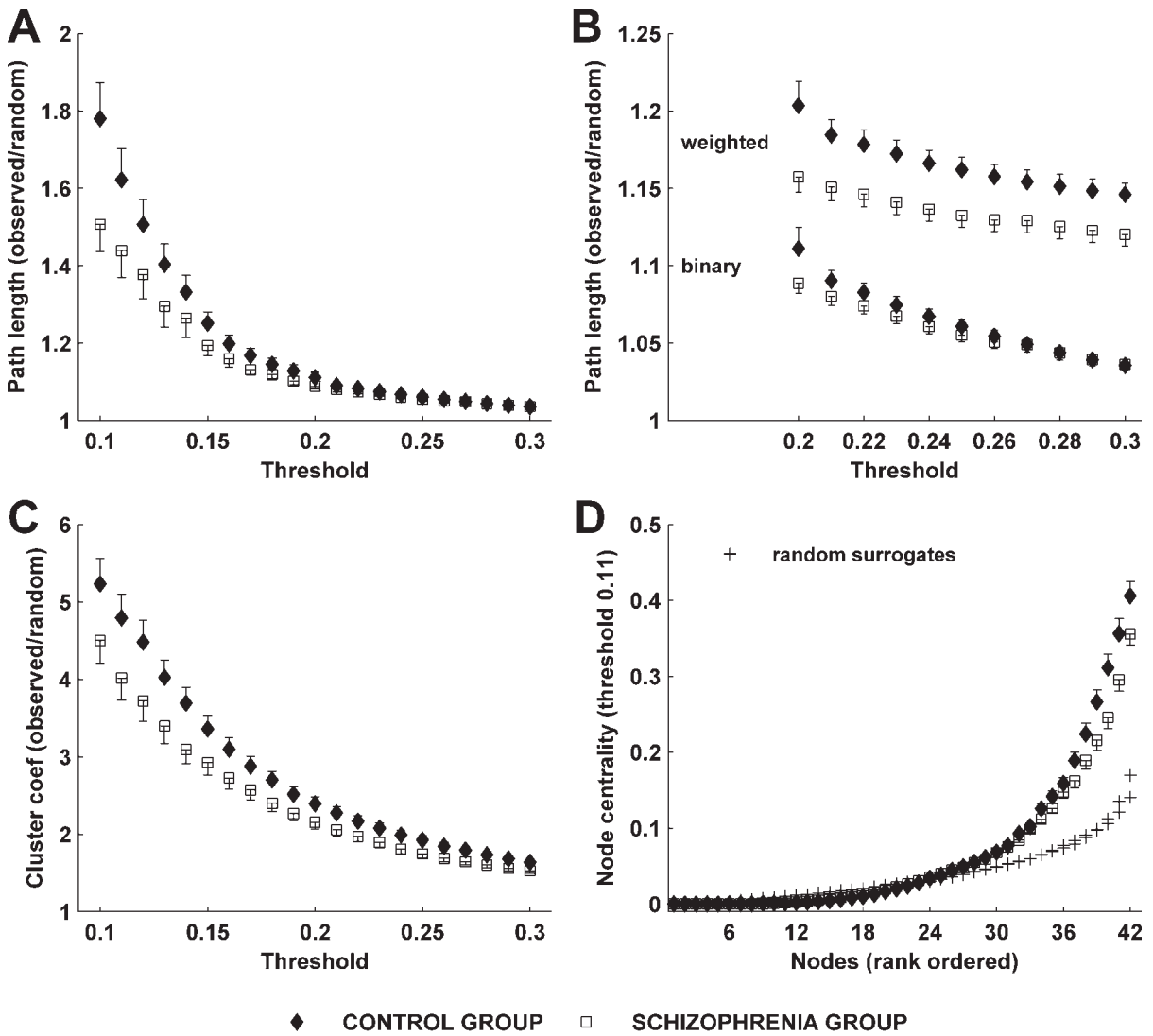

Figure 6.

(**A**) Mean normalized path length for binary graphs of both subject groups. (**B**) A comparison of binary and weighted path lengths at thresholds 20–30%. (**C**) Mean normalized clustering coefficients for binary graphs of both subject groups. (**D**) Mean rank-ordered centrality indices for binary graphs of both subject groups at threshold 12%.

a much greater discriminatory capacity over a wider range of thresholds. Although trends are still apparent in the binary graphs, retaining the weights of edges is clearly important to our between-group statistical analyses. Therefore the subtle organization of the weights in our graphs provides information additional to the overall topography of edges.

DISCUSSION

We present a detailed analysis of the nonlinear expression of functional connectivity in schizophrenia, by combining time series and graph-theoretical methods. By calculating the covariation of nonlinear interdependence in multivariate data, the present method captures the complex topography of cortical interactions, as mapped into scalp EEG, during a resting state condition. Graph measures characterized this topography, reducing the original EEG data set into a few summary statistics. We hence find lower clustering, shorter path lengths and lower centrality of major hubs in the schizophrenia networks. All of these findings are consistent with a subtle randomization of the networks, moving edges away from clustered cliques, creating shortcuts between clusters and hence reducing the centrality of hubs. These findings complement a recent study of linear and nonlinear effects in schizophrenia during a working memory task [Micheloyannis et al., 2006] and are interpreted in two contexts: the schizophrenia disconnection hypothesis, and the study of functional connectivity with graph-theoretical methods.

Our primary purpose was to employ nonlinear measures of interdependence to test the schizophrenia "disconnection hypothesis" [Andreasen, 1999; Friston and Frith, 1995; Lee et al., 2003; Peled, 1999]. However, instead of considering synchronous activity between pairs of cortical areas (a straightforward interpretation of functional connectivity), we studied the temporal correlation of such activities. The nodes in our graphs constitute interdependences between two cortical regions ("first-order" connectivities); the edges correspond to the correlations between pairs of such interdependences ("second-order" connectivities). This measure is sensitive to the location and relative timing of cortical interactions (which are averaged out in first order analyses). By capturing the patterns of synchronous brain activity at a larger, supra-regional scale, it is therefore directed at the evaluation of higher-order integrative processes, rather than of simple inter-regional communication. An increase in the temporal correlation of interdependences was previously reported in schizophrenia, across mostly adjacent interdependence pairs [Breakspear et al., 2003]. Here we confirm this pattern in an expanded dataset, which incorporates a greater number of nonadjacent (disjoint) interdependence pairs. In addition we report that the increase in these correlations in schizophrenia is associated with a randomization in their topographical pattern ("network structure"). The essence of this randomization may be reflected by the average matrices of both networks (Fig. 3B). An important difference between the matrices is the relative increase in the number of intercluster edges in schizophrenia and hence the decrease of edges present inside clusters. These intercluster edges represent the simultaneous occurrence of pairs of "disjoint" nonlinear brain activities. Their increased number corresponds to an increased concurrent occurrence of "remote" dynamical interactions. Put alternatively, these edges reflect a temporal "binding" (cooccurrence) of nonlinear effects which are both spatially and temporally disjoint in healthy subjects. Peled [1999] proposed that the symptoms in schizophrenia may reflect the breakdown of multiple constraint organization (MCO) in the brain, whereby all subcomponents of a system comply with "constraints" exerted by other components. One type of MCO breakdown involves the presence of false connections, which "enable the formation of associations that were impossible before constraints were violated" [Peled, 1999]. Lee et al. [2003] introduced the notion of "overbinding"—the formation of excessive connections that are effectively random—and, in addition, do not distinguish external from internal sources. Our results offer support for these proposals, consistent with Friston and Frith's [1995] notion of a "subtle but pernicious" disturbance.

Our finding of small-world properties in cortical network activity accords with recent analyses of fMRI [Achard et al., 2006; Salvador et al., 2005] and MEG data [Bassett et al., 2006] in addition to computational simulations of cortical activity [Honey et al., 2007]. Recent graph analyses of functional connectivity in EEG reported a randomization of such network structure in brain tumors [Bartolomei et al., 2006] and a loss of small-world network properties in Alzheimer's disease [Stam et al., 2007], interictal state of temporal lobe epilepsy [Ponten et al., 2007] and schizophrenia [Micheloyannis et al., 2006]. The latter study examined the graph properties of linear and nonlinear "first-order" connectivities in band-pass filtered data. The analysis was hence directed towards different properties of EEG data than the present study. The Micheloyannis study reported a lower clustering coefficient—as in the present study—but a longer path length in schizophrenia. A direct comparison between these frequency band specific findings and our current analysis is not possible. However, both analyses also argue that schizophrenia is associated with differences in neuronal dynamics expressed at the scale of the whole brain.

An intriguing finding of the present study is the significant correlation between clustering coefficients and antipsychotic medication dose within the clinical group. This correlation was in the opposite direction of the main intergroup effect, and was independent of crude measures of disease severity (aggregate positive and aggregate negative symptom ratings). There was no clear delineation of subjects into subgroups based on network structure, to account for such a correlation. This result suggests that medication is unlikely to be a confounding factor and may on the contrary exert a "normalizing" influence against the randomization in network structure.

We did not find any meaningful correlations between network structure and symptom ratings on the PANSS. We previously found a lack of fit in this group to either a three-factor or a four-factor model, following a principal components analysis of the symptom ratings [Breakspear et al., 2003]. Both these observations may speak to the acute nature and recent onset of the illness in the group. More specific associations between symptom profiles and patterns of disconnection may emerge with illness chronicity, as suggested by linear connectivity studies showing global loss of synchrony in first episode schizophrenia that—with illness chronicity—acquires specific associations with positive and negative symptom profiles [e.g. Lee et al., 2003; Symond et al., 2005].

Other possible confounding factors, including group differences in arousal and eye movement were addressed in Breakspear et al. [2003]. Here, we readdressed the possibility of confounding by eye movement, as follows: we reanalyzed the networks after excluding frontal region data (Nodes 1–12 in Fig. 3B), and thereby reducing any potential contributions of ocular artifacts. Such a maneuver decreased the number of edges by approximately one half; however, in spite of this, the schizophrenia group networks continued to manifest lower clustering and shorter path lengths at all thresholds. This observation further reduces the possibility of confounding by eye movement.

Previous graph analyses of functional connectivity have, for the most part, considered binary graphs. Weighted graph analysis is a recent development in the study of complex networks [Barrat et al., 2004; Boccaletti et al., 2006]. We found that weighted network analysis revealed a much stronger between-group difference in measurements of both characteristic path length and clustering coefficient (see Fig. 6). This may be explained by the fact that, in more densely connected graphs, there exists a greater presence of weaker edges (corresponding to less significant correlations). In weighted graphs weak edges are less likely to participate in shortest paths, and are therefore less likely to facilitate erroneous long-distance shortcuts which obscure path length differences. Likewise, weak edges have a comparatively smaller influence on the weighted clustering coefficient. In binary graphs all edges have equivalent weights, and the addition of more edges may enable an abundance of short paths and nonclustered neighborhoods, which reduces the overall network metrics, and obscures the between-group difference in our data. In other words, weighted analysis may naturally "filter out" the noise of weaker edges in calculations of path length and clustering coefficient. This argues for the use of weighted rather than the more popular binary graph analyses in future studies.

We found that individual subjects had strongly central hubs. However, we did not observe a robust topographic distribution of hubs across subjects (compare Fig. 5A,B). This may reflect the nature of a "no task" resting state data set, whereby the range of putative cognitive activity between subjects—varying from visual imagery through episodic memory retrieval to executive planning—is far less constrained than during an active cognitive task. Despite this, recent analyses of resting state fMRI data sets do show a remarkably robust pattern of "default mode" activity [Damoiseaux et al., 2006]. However, such networks have very slow oscillations of ~0.05 Hz [Achard et al., 2006] in comparison to the relatively fast time scales of nonlinear EEG activity of 10–40Hz [Breakspear and Terry, 2002a] which may be more closely related to cognitive activity and hence more variable in resting state data. Hence—according to the present analysis—individual subjects' EEG do express hubs during a resting state acquisition, albeit in subject-specific patterns. The schizophrenia group manifested comparatively less central hubs, consistent with a partial randomization of network topography.

In summary, we report a significant random shift in the network structure of resting state EEG in schizophrenia subjects. We interpret this finding as the presence of abnormal synchrony between spatially and temporally disjoint nonlinear activities. These findings do not directly support a "first pass" interpretation of the schizophrenia disconnection hypothesis—whereby cortical regions are simply "uncoupled"—but do support a more complex view of connectivity, whereby cortical interactions are finely balanced between integration and segregation across a hierarchy of scales. This notion is consistent with a recent functional neuroimaging study of Das et al. (in press) which reported a reversal of normal cortical-subcortical interactions. Taken together, these findings hence suggest that schizophrenia is associated with a disturbance in the subtle balance of such hierarchical interactions, up to the scale of the whole brain.

ACKNOWLEDGMENTS

This paper is dedicated to the memory of Alex Rubinov and Claire Breakspear. MR was supported by an SRI Summer Scholarship. MB and SAK were supported by Brain NRG Grant JSM22002082. MB was supported by ARC Grants DP0667065, TS0669860.

REFERENCES

Achard S, Salvador R, Whitcher B, Suckling J, Bullmore E (2006): A resilient, low-frequency, small-world human brain functional network with highly connected association cortical hubs. J Neurosci 26:63–72.

American Psychiatric Association (1994): Diagnostic and Statistical Manual of Mental Disorders: DSM IV. Washington, DC: American Psychiatric Association.

Andreasen NC (1999): A unitary model of schizophrenia: Bleuler's "fragmented phrene" as schizencephaly. Arch Gen Psychiatry 56:781–787.

Andreasen NC, O'Leary DS, Cizadlo T, Arndt S, Rezai K, Ponto LL, Watkins GL, Hichwa RD (1996): Schizophrenia and cognitive dysmetria: A positron-emission tomography study of dysfunctional prefrontal-thalamic-cerebellar circuitry. Proc Natl Acad Sci USA 93:9985–9990.

Andreasen NC, Nopoulos P, O'Leary DS, Miller DD, Wassink T, Flaum M (1999): Defining the phenotype of schizophrenia:

Cognitive dysmetria and its neural mechanisms. Biol Psychiatry 46:908–920.

Arnhold J, Grassberger P, Lehnertz K, Elger CE (1999): A robust method for detecting interdependences: Application to intracranially recorded EEG. Phys D 134:419–430.

Barrat A, Barthelemy M, Pastor-Satorras R, Vespignani A (2004): The architecture of complex weighted networks. Proc Natl Acad Sci USA 101:3747–3752.

Bartolomei F, Bosma I, Klein M, Baayen JC, Reijneveld JC, Postma TJ, Heimans JJ, van Dijk BW, de Munck JC, de Jongh A, Cover KS, Stam CJ (2006): Disturbed functional connectivity in brain tumours patients: Evaluation by graph analysis of synchronization matrices. Clin Neurophysiol 117:2039–2049.

Bassett DS, Bullmore E (2006): Small-world brain networks. Neuroscientist 12:512–523.

Bassett DS, Meyer-Lindenberg A, Achard S, Duke T, Bullmore E (2006): Adaptive reconfiguration of fractal small-world human brain functional networks. Proc Natl Acad Sci USA 103:19219–19220.

Bleuler E (1911/1950): Dementia Praecox or the Group of Schizophrenias. New York: International Universities Press.

Boccaletti S, Latora V, Moreno Y, Chavez M, Hwang DU (2006): Complex networks: Structure and dynamics. Phys Rep 424: 175–308.

Breakspear M (2004): "Dynamic" connectivity in neural systems: Theoretical and empirical considerations. Neuroinformatics 2:205–226.

Breakspear M (2006): The nonlinear theory of schizophrenia. Aust N Z J Psychiatry 40:20–35.

Breakspear M, Terry JR (2002a): Detection and description of nonlinear interdependence in normal multichannel human EEG data. Clin Neurophysiol 113:735–753.

Breakspear M, Terry JR (2002b): Topographic organization of nonlinear interdependence in multichannel human EEG. NeuroImage 16:822–835.

Breakspear M, Terry JR, Friston KJ, Harris AW, Williams LM, Brown K, Brennan J, Gordon E (2003): A disturbance of nonlinear interdependence in scalp EEG of subjects with first episode schizophrenia. NeuroImage 20:466–478.

Breakspear M, Roberts JA, Terry JR, Rodrigues S, Mahant N, Robinson PA (2006): A unifying explanation of primary generalized seizures through nonlinear brain modeling and bifurcation analysis. Cereb Cortex 16:1296–1313.

Bullmore ET, Frangou S, Murray RM (1997): The dysplastic net hypothesis: An integration of developmental and dysconnectivity theories of schizophrenia. Schizophr Res 28:143–156.

Damoiseaux JS, Rombouts SA, Barkhof F, Scheltens P, Stam CJ, Smith SM, Beckmann CF (2006): Consistent resting-state networks across healthy subjects. Proc Natl Acad Sci USA 103:13848–13853.

Das P, Kemp AH, Flynn G, Harris AW, Liddell BJ, Whitford TJ, Peduto A, Gordon E, Williams LM (2007): Functional disconnections in the direct and indirect amygdala pathways for fear processing in schizophrenia. Schizophr Res 90:284–294.

Freeman LC (1977): A set of measures of centrality based on betweenness. Sociometry 40:35–41.

Friston KJ (2001): The labile brain. I. Neuronal transients and nonlinear coupling. Phil Trans R Soc Lond B 355:215–236.

Friston KJ, Frith CD (1995): Schizophrenia: A disconnection syndrome? Clin Neurosci 3:89–97.

Gottschalk A, Bauer MS, Whybrow PC (1995): Evidence of chaotic mood variation in bipolar disorder. Arch Gen Psychiatry 52:947–959.

Gratton G, Coles MG, Donchin E (1983): A new method for offline removal of ocular artifact. Electroencephalogr Clin Neurophysiol 55:468–484.

Greicius MD, Krasnow B, Reiss AL, Menon V (2003): Functional connectivity in the resting brain: A network analysis of the default mode hypothesis. Proc Natl Acad Sci USA 100:253–258.

Haig AR, Gordon E, De Pascalis V, Meares RA, Bahramali H, Harris A (2000): Gamma activity in schizophrenia: Evidence of impaired network binding? Clin Neurophysiol 111:1461–1468.

Harris A, Brennan J, Anderson J, Taylor A, Sanbrook M, Fitzgerald D, Lucas S, Redoblado-Hodge A, Gomes L, Gordon E (2005): Clinical profiles, scope and general findings of the Western Sydney First Episode Psychosis Project. Aust N Z J Psychiatry 39:36–43.

He Y, Chen ZJ, Evans AC (2007): Small-world anatomical networks in the human brain revealed by cortical thickness from MRI. Cereb Cortex 17:2407–2419.

Honey C, Kötter R, Breakspear M, Sporns O (2007): Network structure of cerebral cortex shapes functional connectivity on multiple time scales. Proc Natl Acad Sci USA 104:10240–10245.

Humphries MD, Gurney K, Prescott TJ (2006): The brainstem reticular formation is a small-world, not scale-free, network. Proc Biol Sci 22:503–511.

Jirsa VK, Fuchs A, Kelso JA (1998): Connecting cortical and behavioral dynamics: Bimanual coordination. Neural Comput 10:2019–2045.

Kay SR, Opler LA, Fiszbein A (1986): Positive and negative syndrome scale (PANSS). North Tonawanda, NY: Multi-Health Systems Inc.

Lee KH, Williams LM, Breakspear M, Gordon E (2003): Synchronous gamma activity: A review and contribution to an integrative neuroscience model of schizophrenia. Brain Res Rev 41:57–78.

Marchiori M, Latora V (2000): Harmony in the small-world. Phys A 285:539–546.

Maslov S, Sneppen K (2002): Specificity and stability in topology of protein networks. Science 296:910–913.

Meyer-Lindenberg A, Ziemann U, Hajak G, Cohen L, Berman KF (2002): Transitions between dynamical states of differing stability in the human brain. Proc Natl Acad Sci USA 20:10948–10953.

Micheloyannis S, Pachou E, Stam CJ, Breakspear M, Bitsios P, Vourkas M, Erimaki S, Zervakis M (2006): Small-world networks and disturbed functional connectivity in schizophrenia. Schizophr Res 87:60–66.

Milo R, Shen-Orr S, Itzkovitz S, Kashtan N, Chklovskii D, Alon U (2002): Network motifs: Simple building blocks of complex networks. Science 298:824–827.

Newman MEJ (2003): The structure and function of complex networks. SIAM Rev 45:167–256.

Nunez PL, Srinivasan R, Westdorp AF, Wijesinghe RS, Tucker DM, Silberstein RB, Cadusch PJ (1997): EEG coherency. I: Statistics, reference electrode, volume conduction, Laplacians, cortical imaging, and interpretation at multiple scales. Electroencephalogr Clin Neurophysiol 103:499–515.

Peled A (1999): Multiple constraint organization in the brain: A theory for schizophrenia. Brain Res Bull 49:245–250.

Perez Velazquez JL, Khosravani H (2004): A subharmonic dynamical bifurcation during in vitro epileptiform activity. Chaos 14:333–342.

Ponten SC, Bartolomei F, Stam CJ (2007): Small-world networks and epilepsy: Graph theoretical analysis of intracerebrally recorded mesial temporal lobe seizures. Clin Neurophysiol 118:918–927.

Prichard D, Theiler J (1994): Generating surrogate data for time series with several simultaneously measured variables. Phys Rev Lett 73:951–954.

Rabinovich MI, Huerta R, Varona R (2006): Heteroclinic synchronization: Ultrasubharmonic locking. Phys Rev Lett 96:14101.

Rombouts SARB, Keunen RWM, Stam CJ (1995): Investigation of nonlinear structure in multichannel EEG. Phys Lett A 202:352–358.

Roskies AL (1999): The binding problem. Neuron 24:111–125.

Salvador R, Suckling J, Coleman MR, Pickard JD, Menon D, Bullmore E (2005): Neurophysiological architecture of functional magnetic resonance images of human brain. Cereb Cortex 15:1332–1342.

Schanze T, Eckhorn R (1997): Phase correlation among rhythms present at different frequencies: Spectral methods, application to microelectrode recordings from visual cortex and functional implications. Int J Psychophysiol 26:171–189.

Schiff SJ, So P, Chang T, Burke RE, Sauer T (1996): Detecting dynamical interdependence and generalized synchrony through mutual prediction in a neural ensemble. Phys Rev E 54:6708–6724.

Spencer KM, Nestor PG, Niznikiewicz MA, Salisbury DF, Shenton ME, McCarley RW (2003): Abnormal neural synchrony in schizophrenia. J Neurosci 23:7407–7411.

Sporns O, Zwi JD (2004): The small world of the cerebral cortex. Neuroinformatics 2:145–162.

Stam CJ, Reijneveld JC (2007): Graph theoretical analysis of complex networks in the brain. Nonlinear Biomed Phys 1:3.

Stam CJ, Pijn JP, Suffczynski P, Lopes da Silva FH (1999): Dynamics of the human alpha rhythm: Evidence for non-linearity? Clin Neurophysiol 110:1801–1813.

Stam CJ, Jones BF, Nolte G, Breakspear M, Scheltens Ph (2007): Small-world networks and functional connectivity in Alzheimer's disease. Cereb Cortex 17:92–99.

Stephan KE, Hilgetag CC, Burns GA, O'Neill MA, Young MP, Kotter R (2000): Computational analysis of functional connectivity between areas of primate cerebral cortex. Philos Trans R Soc Lond B Biol Sci 355:111–126.

Symond M, Harris AWF, Gordon E, Williams LM (2005): "Gamma synchrony" in first-episode schizophrenia: A disorder of temporal connectivity? Am J Psychiatry 162:459–465.

Terry JR, Breakspear M (2003): An improved algorithm for the detection of dynamical interdependence in bivariate time-series. Biol Cybern 88:129–136.

Tononi G, Edelman GM (2000): Schizophrenia and the mechanisms of conscious integration. Brain Res Rev 31:391–400.

Tononi G, Sporns O, Edelman GM (1994): A measure for brain complexity: Relating functional segregation and integration in the nervous system. Proc Natl Acad Sci USA 91:5033–5037.

Tschacher W, Scheier C, Hashimoto Y (1997): Dynamical analysis of schizophrenia courses. Biol Psychiatry 41:428–437.

Watts DJ, Strogatz SH (1998): Collective dynamics of "small-world" networks. Nature 393:440–442.

Williams LM, Loughland CM, Gordon E, Davidson D (1999): Visual scanpaths in schizophrenia: Is there a deficit in face recognition? Schizophr Res 40:189–199.

Woodruff PW, Wright IC, Shuriquie N, Russouw H, Rushe T, Howard RJ, Graves M, Bullmore ET, Murray RM (1997): Structural brain abnormalities in male schizophrenics reflect fronto-temporal dissociation. Psychol Med 27:1257–1266.

APPENDIX

MATHEMATICAL DETAILS OF WEIGHTED GRAPH ANALYSIS

The present study utilized weighted, undirected graphs. A weighted, undirected graph $G^W = (V, E, W)$ consists of three sets: a nonempty set of vertices, or nodes, V (comprising N nodes); a set of edges E; and a set of edge weights W. Nodes i and j (here and in the following $i, j \in V$) are said to be adjacent ($a_{ij} = 1$) when there exists an edge between i and j; and nonadjacent ($a_{ij} = 0$) otherwise, with $a_{ij} = a_{ji}$ and $a_{ii} = 0$ for all i and j. All adjacent i and j are assigned an edge weight w_{ij}, with $0 < w_{ij} \leq 1$ and $w_{ij} = w_{ji}$; all nonadjacent i and j have $w_{ij} = 0$.

Clustering Coefficient [Barrat et al., 2004]

The binary clustering coefficient c_i^w of a node i, is the likelihood of $a_{jh} = 1$, if $a_{ij} = a_{ih} = 1$. Thus, $c_i = \frac{1}{k_i(k_i-1)} \sum_{j \neq h \in V} a_{ij} a_{ih} a_{jh}$, where k_i is the number of neighbors (degree) of i, $k_i = \sum_{j \in V} a_{ij}$. The weighted clustering coefficient c_i^w, incorporates node-neighbor weights as, $c_i^w = \frac{1}{s_i(k_i-1)} \sum_{j,h \in V} \frac{(w_{ij}+w_{ih})}{2} a_{ij} a_{ih} a_{jh}$, where s_i is the weighted degree (strength) of i, $s_i = \sum_{j \in V} w_{ij}$. The average clustering coefficient C, is obtained as, $C = \frac{1}{N} \sum_{i \in V} c_i$.

Characteristic Path Length [Marchiori and Latora, 2000]

We obtained shortest path lengths d_{ij} between nodes i and j, by taking distance to be inversely proportional to weight. For disconnected nodes, we assumed $d_{ij} = \infty$. The characteristic path length L, was derived as a harmonic mean of the individual shortest path lengths, $L = \frac{N(N-1)}{\sum_{i,j \in V} 1/d_{ij}}$.

Betweenness Centrality [Freeman, 1977]

Betweenness centrality b_i of a node i, is the sum of the ratios of the number of shortest paths traversing i, $b_i = \sum_{i \neq j \neq h \in V} \frac{n_{jh}(i)}{n_{jh}}$, where n_{jh} is the number of shortest paths between j and h, and $n_{jh}(i)$ is the number of shortest paths between j and h that traverse i. Betweenness was normalized as, $b_i^{nml} = \frac{b_i}{(N-1)(N-2)}$.